# Transcritical and Supercritical Fuel Sprays in Subcritical Environments

Robert Kempin<sup>1</sup>, Kaushik Nonavinakere Vinod<sup>1</sup>, Owen Morris<sup>1</sup>, and Tiegang Fang<sup>\*1</sup>

<sup>1</sup>Dept. of Mechanical and Aerospace Engineering, North Carolina State University, Raleigh, NC, USA

#### **Abstract**

As fuel injection systems advance towards higher injection pressures and the combustor environment increases in both temperature and pressure in the pursuit of improved emissions and efficiency, advanced combustion strategies are required. Injecting fuel as a supercritical fluid has the potential to improve fuel/air mixing and eliminate steps in the spray vaporization process. Experiments are carried out on a heated fuel injector in an open-air test cell using Mie scattering, Schlieren imaging, and long-distance microscopy to investigate changes in spray characteristics with varying temperature and pressure. Spray angle, spray penetration length, and vapor-liquid ratio data are collected and evaluated. Near-nozzle imaging shows distinct changes in spray morphology during the initial microseconds of spray formation. Sprays injected under conditions further into the supercritical regime exhibit increased spray angle and vapor-to-liquid ratio. Spray penetration is found to decrease with increasing temperature. A jump in vapor-to-liquid ratio is observed in the vicinity of 568 K. indicating a transition in spray behaviour trending towards more rapid fuel/air mixing across the transcritical region. Changes in the micro-scale structure of the spray during the initial microseconds of spray formation exhibit this same narrow transition region. A significantly greater fraction of the spray plume is observed to be in a vapor or vapor-like state at a given time after injection initiation as the injection conditions are advanced into the supercritical state. These findings indicate that injection fuel as a supercritical fluid has the potential to improve the mixing of a fuel/air charge, and thus, improve combustion quality.

## **Keywords**

Supercritical spray, Supercritical fluids, Flash boiling, Fuel injection

## Introduction

In the face of ever more stringent emissions regulations, there is a clear need for advanced combustion strategies in internal combustion engines (ICEs) to improve efficiency while reducing pollutant formation.

In-cylinder improvements to ICE emissions and combustion efficiency are in large part driven by the fuel spray characteristics. Spray quality directly impacts engine performance and efficiency through improved mixing and combustion characteristics. More desirable spray characteristics may be obtained through increased injection pressure. Morgan et al. demonstrated the need for injection pressures in excess of 240 MPa in order to improve the trade-off between NOx and fuel consumption in compression ignition (CI) engines [1]. They also note that under low/medium loads the parasitic work of such high injection pressure reduces overall engine performance. Chen et al. showed that increasing injection pressure is effective for reducing droplet diameter for diesel fuel, biodiesels, and Jet-A kerosene[2]. High pressure injection systems further provide a more uniform radial distribution of droplet size [2,3]. These improvements in atomization lead to faster fuel-air mixing as shown by Yao et al. in a constant volume combustion chamber (CVCC) [4]. Faster combustion rates and a shorter ignition delay are thus observed. Experiments at ultra-high pressures show that shock waves generated by the supersonic jet contribute to this improved breakup [6,5].

Supercritical fluids (SCFs) are of interest due to the unique physical properties they exhibit. In an SCF, the surface tension of the fluid and the latent heat of evaporation approach nil. Conventional liquid spray breakup d oes not occur, rather, the SCF jet dissipates into the ambient much as would be expected of a gas jet. This, combined with maxima in various thermodynamic properties in the vicinity of the critical point, indicates that a supercritical fluid may in a sense be 'tuned' to obtain more favourable behaviour for a given purpose.

One challenge of studying SCF sprays is the problem of adapting existing optical techniques to accurately differentiate the states being observed. Work to evaluate the optical properties of droplets near and past the critical point has been performed by Kanjanasakul et al. on transcritical ethanol droplets, developing a technique based on rainbow refractometry capable of measuring both vapor concentration near the droplet as well as refractive index and droplet diameter [7]. Strong concentration gradients also present schlieren imaging as a powerful technique for analysis of spray formation [8,10,9]. Laser doppler velocimetry (LDV) techniques are used by Gallarini et al. to directly measure velocity fields in high-temperature, non-ideal flows to include SCF flows [11].

Experimental work has been conducted in recent years to study the behaviour of SCF sprays of various fuels under varying conditions, largely investigating dense-fluid jet behaviour. Systems studied can be broadly broken down into diesel-type, rocket-type, and single gas type. Dahms and Oefelein define three mixing regimes based on Knudsen number in a rocket-type system, these being classical spray, diffusion dominated mixing, and supercritical mixing [12]. They further conclude that the mixing mechanism depends heavily on injection conditions, and less so on environmental conditions. Yang et al. studied phase transition of CO<sub>2</sub> jets in varying atmospheres, finding that supercritical sprays behaved in many ways as a gas jet and observing an increase in radial spreading under transcritical conditions [13]. Rezaei et al. investigated phase change under diesel-type conditions, finding that heat transfer rates under elevated pressure and temperature ambient conditions are sufficient for the fuel jet to reach supercritical temperature before mixing prevents such [14]. This reinforces the observations by Crua et al. that at elevated ambient conditions classical evaporation was replaced by diffusive mixing in individual fuel droplets [15]. Work on transcritical phase changes in diesel conditions has been done by the same group in Riess et al. and further reinforced the relevance of heat transfer dominated mixing as well as modelling the relevant thermodynamic processes [14]. Further studies on mixing have established temperature thresholds working in an ethanol/N<sub>2</sub> system for fully supercritical sprays, showing that ambient temperature in excess of the fuel critical temperature is insufficient for supercritical spray mixing [16].

Computational work has been conducted to model the behaviour of dense fluid behaviour in systems ranging from single droplet to turbulent combustion in a simulated combustion chamber. Molecular dynamics simulations have demonstrated the change from evaporative to diffusive mixing with increasing temperature and pressure [17,18]. Multiple groups have simulated supercritical sprays and/or spray combustion in the context of an ICE [20,23,24,21,22,19]. Zhang et al. modelled the multiphase thermodynamics of supercritical CO<sub>2</sub> systems, finding that both small differences in mixture composition and fluid mixing effects can drastically alter the critical point of the working fluid [25].

The work at hand investigates spray characteristics of Jet-A1 fuel injected into room temperature and pressure conditions. The fuel injected is pressurized to well in excess of the critical pressure and the injector tip is heated, raising the fuel inside the tip past the critical

point. Sprays in which the fuel exists within the subcritical, transcritical, and supercritical regimes are investigated using Schlieren imaging and Mie scattering. Near nozzle effects are studied using long-distance microscopy.

## **Experimental setup**

Sprays of Jet-A1 fuel were evaluated by injection at elevated pressure and temperature into air at room temperature and pressure. Doing such allows for unrestricted optical access to the spray, as well as providing a necessary baseline for future work. Two diagnostic techniques were used to separately evaluate the liquid and vapor regions of the spray. Z-type Schlieren imaging allows visualization of the entire spray. The liquid region alone may be viewed by the placement of a LED source normal to both the Schlieren view-path and the spray. The Mie scattering signal is collected by the same camera as the Schlieren signal. Arranging the apparatus in this manner allows for the data sets to be overlaid upon each other for analysis with minimal error.

A common rail fuel injection system drives the injector system. A Bosch CRI Type 2.2 fuel injector is mounted in a heated block. A single-hole nozzle with an orifice diameter of 200 µm in installed. Two 500 W disk heaters provide heating controlled by a Watlow EZ-Zone process controller. Temperature measurement is provided by a thermocouple (K-type, Omega) installed at the tip of the injector nozzle. Sufficient time is allowed between injections for the fuel charge in the nozzle to reach steady-state temperature, making this placement sufficiently accurate. The fuel present in the initial stages of the spray presently under consideration is within the nozzle during the period between sprays. This fuel is sufficiently small in volume that it may be assumed to be in thermal equilibrium with the nozzle and heater block at time of injection. Thus, the injector nozzle contains a region wherein the fuel is in a supercritical state.

Imaging is obtained using a z-type Schlieren apparatus for the macroscopic spray data, while backlit imaging is used for near-nozzle imaging. A Phantom VEO710 high speed camera is used to obtain high-speed video footage. Light from a red LED (ThorLabs M625L2) is passed through a pinhole and directed by a pair of parabolic mirrors. An Infinity K2 DistaMax long distance microscope lens is used for the near-nozzle imaging while a Nikon 85mm lens is used for all other imaging. Fig. 1 shows a representative example of macroscopic spray images, both separate and overlaid. Near-nozzle images are shown later in the work.

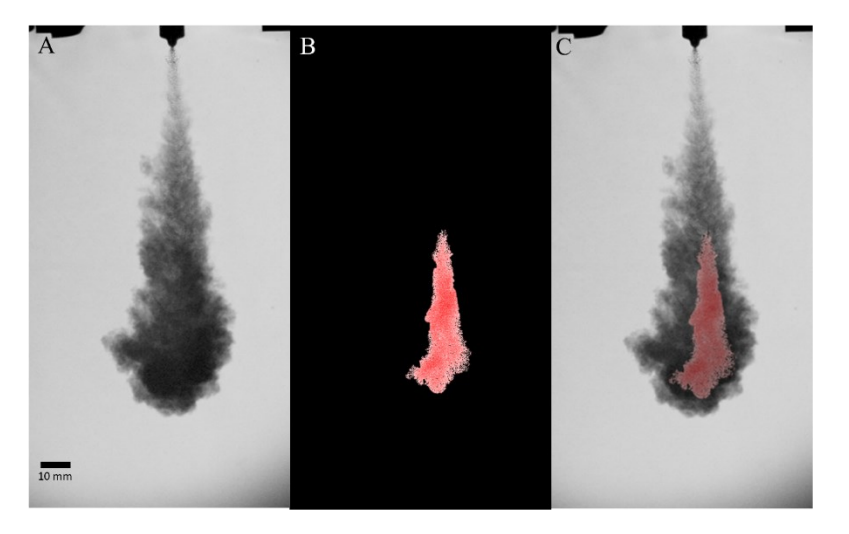


**Figure 1** Representative macroscopic spray at 603 K and 150 MPa injection pressure showing A) Schlieren image B) Mie scattering signal and C) Mie scattering signal overlaid atop the schlieren image.

For the near-nozzle imaging, in order to obtain useful resolutions, the maximum frame rate of the Phantom VEO 710 is insufficient. To bypass this problem, the camera trigger timing is manipulated to simulate a higher frame rate by imaging multiple, statistically similar, sprays at separate times. The camera trigger is advanced in 1-2 µs steps to assemble a composite image. This procedure is repeated until the spray reaches the bottom of the frame. To ensure all sprays are similar, the injector is cycled five times, with the fifth injection being recorded – termed an injection sequence henceforth. This clears the residual fuel out of the injector tip, ensuring a spray which is repeatable enough to establish trends in spray behavior. The cases selected in this work were picked based on initial results from macroscopic data indicating the region of critical transition.

Simultaneous Mie scattering and Schlieren data are gathered at the following operating conditions shown in Fig. 2. For all cases the temperature is the nozzle tip temperature, and injection pressure is the pressure in the common rail system as measured from the fuel rail. Uncertainties in experimental conditions arise from the accuracy of the pressure transducer and thermocouples used in this experiment. The fuel rail pressure transducer used in the experiments has an uncertainty of ±2 bar while the thermocouples and the temperature controller used in the injector heater has a total uncertainty of ±2 K. At each case, six injection sequences are imaged macroscopically and three microscopically, with reported spray angle and penetration being the average of these measurements. This reduces the likelihood of spray-to-spray differences impacting the calculated results.

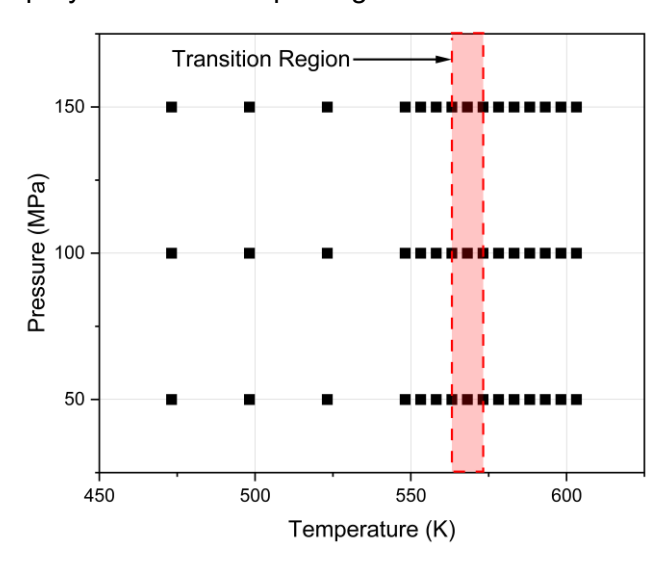


Figure 2 Experimental cases with region of observed transition in spray behaviour highlighted.

## **Results and Discussions**

Directly apparent from Schlieren imaging is the change in spray behavior with increasing temperature. This is shown in Fig. 3, where the spray is significantly less dense. What is a predominately liquid spray in the lower temperature cases has transitioned to a predominately vapor spray once a temperature of 603 K is reached. This is reflected in the increase in vapor to liquid ratio (VLR) with increasing temperature, shown later in the discussion in Fig. 6. With increasing temperature, the liquid region is greatly reduced, despite a similar overall spray size. At higher injection pressures, this effect is more pronounced with a more marked difference between low and high temperature sprays. Thus, it is indicated that increasing injection pressure and temperature has a positive impact upon the vapor to liquid ratio of the spray.

Mean spray angle is presented for select temperature cases in Fig. 4a. Notable trends occur within the first  $500~\mu s$ , roughly, as the heated fuel exits the injector. As the spray progresses, the angle decreases to a mostly steady-state plateau. Here spray breakup transitions from being dominated by diffusive effects towards a pressure driven mode. Indeed, a rapid rise is apparent between the temperatures of 563~K and 573~K, the peak spray angle increasing by 25% within that region. These trends are reflected in the near-nozzle shadowgraph results presented later.

Fig. 4b highlights these trends more clearly by removing the steady state portion of the spray. Made apparent by doing so is the delay in peak spray angle. In subcritical sprays, the spray angle reaches a maximum rapidly after opening. This peak value is not significantly greater than the steady state values, in some cases having a mere 2° of difference. In sprays where supercritical mixing effects are absent, this initial peak is largely due to effects from the opening of the needle. At higher temperatures, the peak is prolonged, indicative of the supercritical fuel diffusing out from the nozzle before the spray becomes dominated by the pressure driven effects and the rapid loss of heat to the atmosphere.

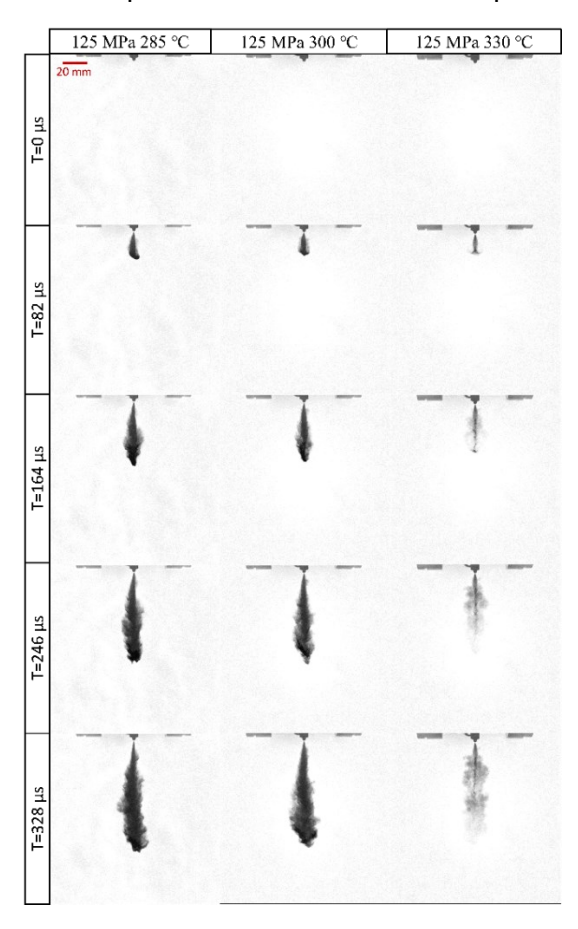
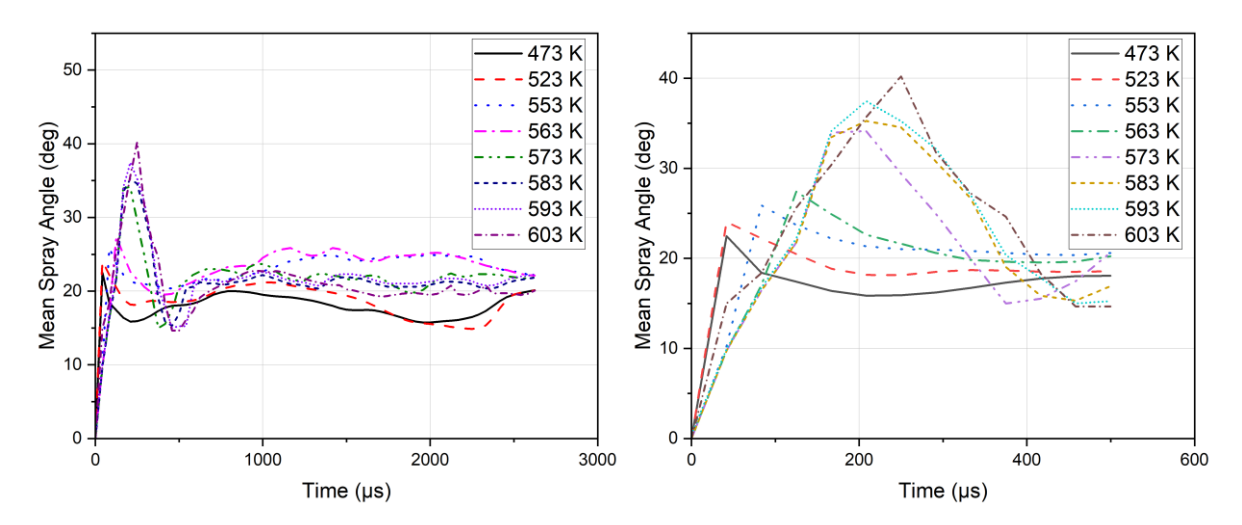


Figure 3 Comparison of supercritical spray evolution at varying conditions.

Even in the supercritical region increases in injection pressure have the expected effect on spray development. Fig. 5 demonstrates this clearly at a high temperature case of 603 K. Though unsurprising, validation of the expected result is of use.



**Figure 4** Mean Spray Angle (MSA) for selected temperature cases at 150 MPa of injection pressure over (a) the full spray duration and (b) the region of peak spray angle.

The vapor liquid ratio (VLR) is obtained through simultaneous analysis of Mie scattering and Schlieren imaging data. Mie scattering shows solely the liquid phase, while Schlieren shows regions of the spray in both the liquid and vapor phases. Through comparison of these two, it is possible to define the relative phase composition of the spray on an area average basis. The VLR was calculated using an imaging setup based on Schlieren and Mie scattering performed on the spray. Using a custom code, the areas of both the schlieren and Mie scattering images were calculated. Since the Schlieren images contain the areas of both the vapor and the liquid phase, and the Mie data shows the area of the liquid phase alone, a difference in both the areas can give us an estimation of the various phases present in the spray. Each spray was repeated a total of 5 times to calculate an average VLR, this data is presented in Fig. 6.

Initially apparent is the clear dependence of VLR on injector temperature. Hotter fuel corresponds to a larger region of the spray in the vapor state as the breakup and mixing of the spray trends towards the diffusion-dominated regime. Additionally, two clear transitions in spray behavior may be observed.

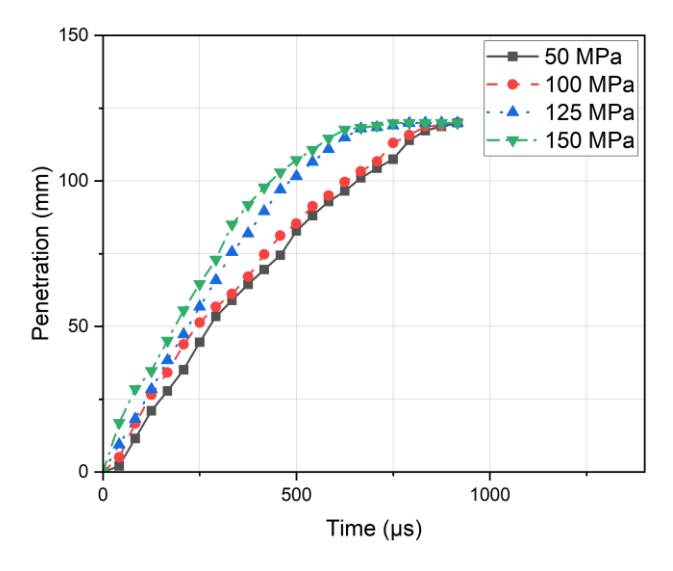


Figure 5 Spray penetration as a function of time at varying pressures at 603 K.

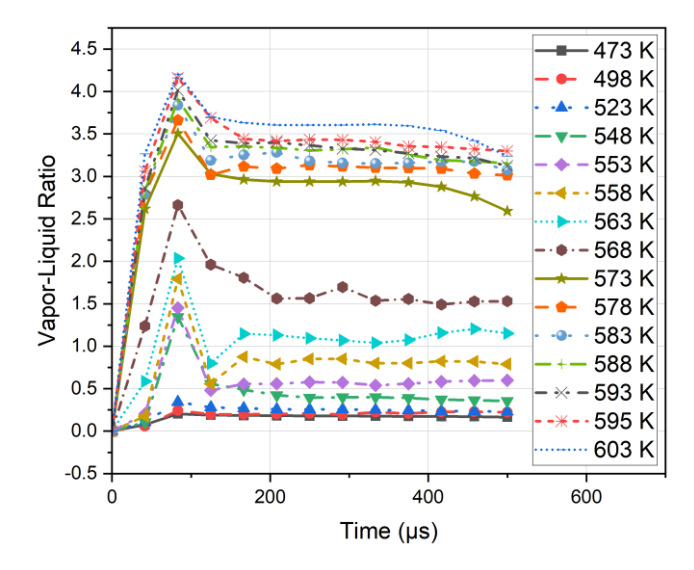
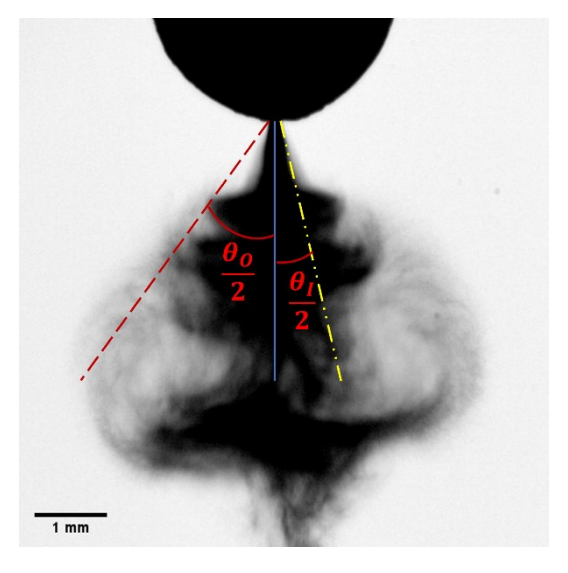


Figure 6 Vapor-Liquid Ratio (VLR) from Mie scattering/Schlieren imaging at injection pressure of 150 MPa.

The first transition may be observed in the peak in VLR which occurs beginning in earnest at a temperature of 548 K. While a minuscule peak is present in lower temperature cases, it is not until the transcritical region of sprays that it is of any significance. Note also that the magnitude of the peak starts to decrease in the high temperature limit of the present data. This indicates a high initial vapor content of the spray, decreasing either as more fuel in the liquid state is injected or as vapor cools and condenses around droplets of liquid fuel remaining in the spray. Hence, the first change in spray behavior is the appearance of this initial peak at around 548 K.

The second transition occurs between 563K and 573 K. A fuel temperature of 563 K results in the VLR steadying out slightly over 1, indicating near equal liquid and vapor presence in the spray. A mere ten degree increase in temperature to 573 K results in a VLR that steadies out around 3, with a peak VLR of 3.5. An injection temperature of 568 K falls neatly within this transition region, albeit slightly more towards the lower end thereof.

The region wherein this transition occurs, as observed in the present dataset, is highlighted in Fig. 2 illustrating the considered test conditions.



**Figure 7** Definition of inner spray angle  $\theta_1$  (dashed, left) and outer spray angle  $\theta_0$  (dot-dash, right).

Evaluation of spray behavior in the very near vicinity of the nozzle during the beginnings of spray formation requires definition of two separate spray angles. Fig. 7 gives the graphical definition of the inner and outer spray angles. The inner spray angle,  $\theta_l$ , is taken as the angle between the spray centerline and the boundary of the pressure-driven core. The outer spray angle,  $\theta_0$ , defines the outermost boundary of the spray. For each case the angle on either side of the centerline is measured, and the results summed. This does not require an assumption of a completely symmetrical spray.

Spray angle trends in this instance are informative. Looking now to Fig. 8 it may be observed that long distance microscopy results do indeed align with macro-scale observations. A larger peak spray angle, developing more rapidly, is observed as the spray conditions approach and cross the critical point. Correspondingly, a decrease in the width of the central, pressure-driven core of the spray may be seen as  $\theta_l$  develops.

Notable however is the middling temperature case of 573 K. Much lower spray angles are observed than in either the subcritical or supercritical case. In particular, the core jet is narrow. The precise reason for this is unclear, warranting further investigation.

Though some quantitative trends do arise from near-nozzle shadowgraph, the ability to observe the early stages of spray development is useful. Within tens of microseconds of observable start of injection differences in spray structure are present with increasing temperature. Fig. 9 illustrates the effects of increasing temperature on spray structure. For reference, an unheated spray is illustrated in Fig. 9A. In particular, comparing Fig. 9D to Figs. 9C & B shows significant change in the spray density. The vapor cloud enveloping the liquid core is visibly less optically dense, indicating more rapid vaporization and diffusive mixing in the vicinity of the nozzle. Here, more fuel is exiting the injector in the supercritical state and is therefore subject to diffusive mixing. Near-supercritical and supercritical cases exhibit enhanced diffusive mixing driven by reduced surface tension and flash boiling effects.

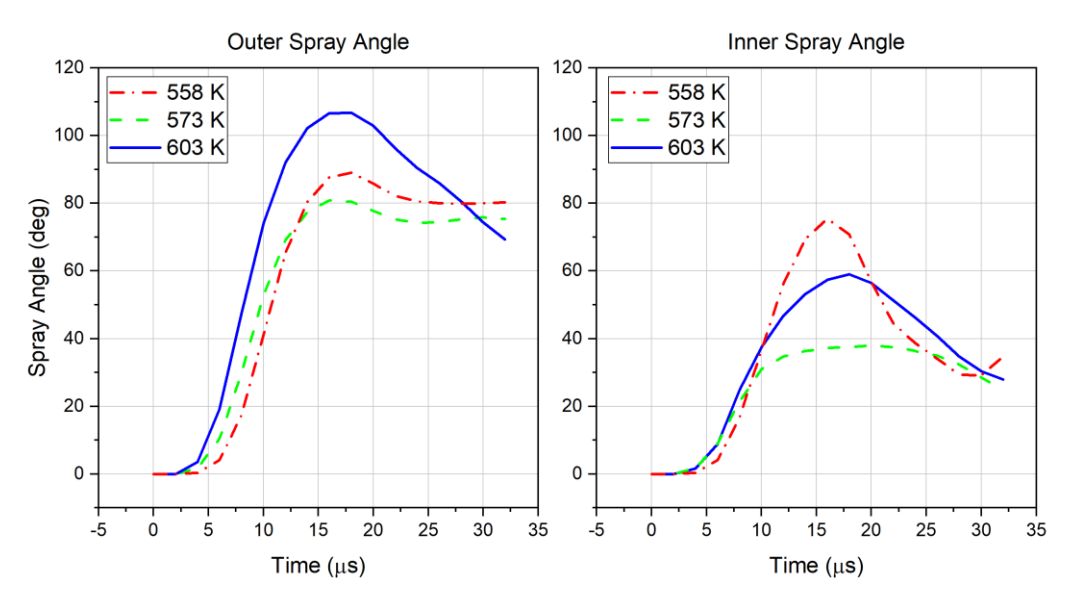


Figure 8 Smoothed and averaged near-nozzle MSA.

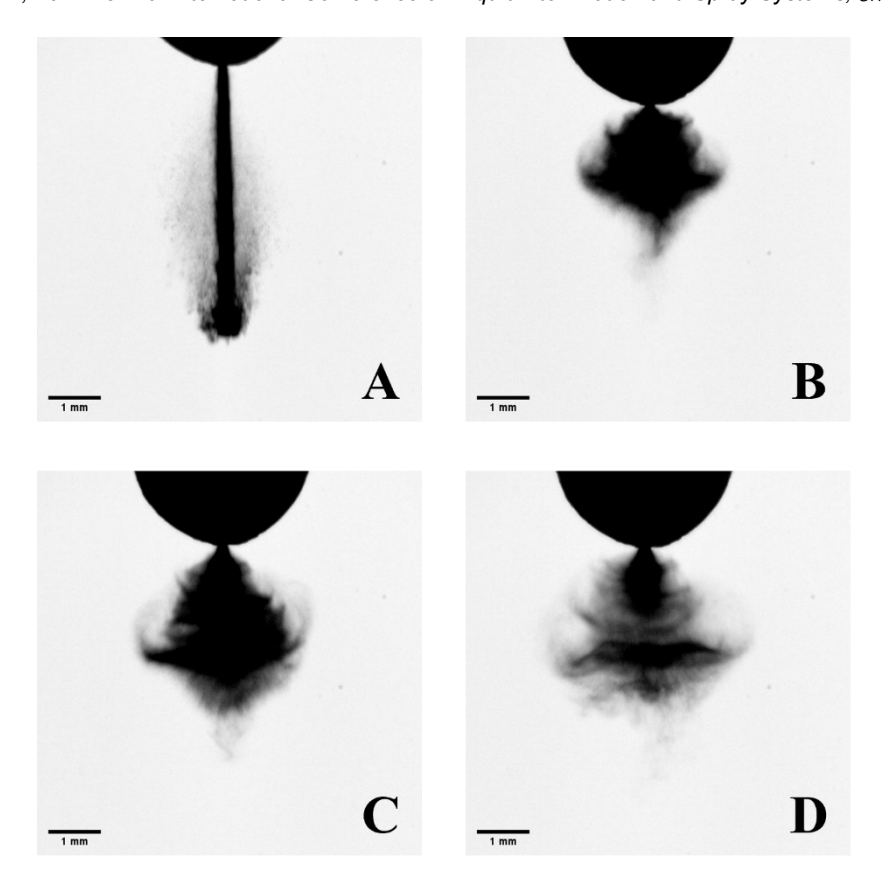


Figure 9 Comparison of sprays 20 µs after injection start A) 293 K; B) 558 K; C) 573 K; D) 603 K.

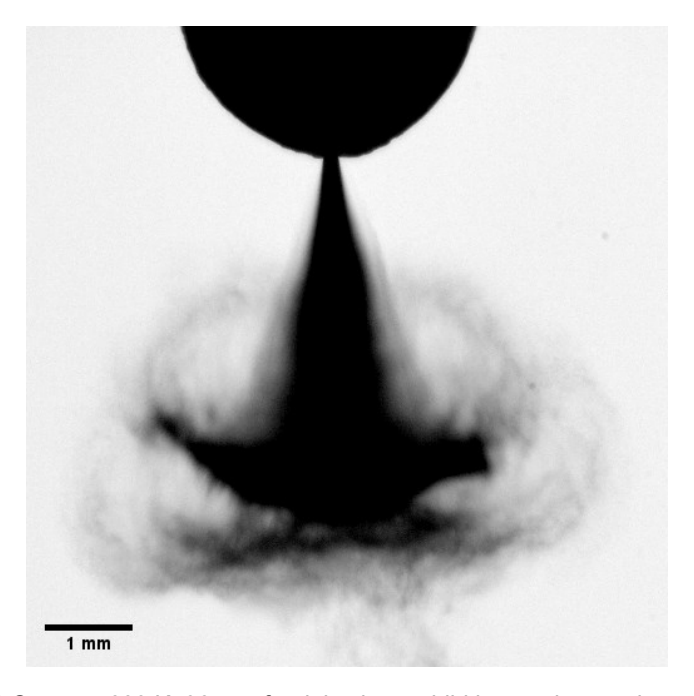


Figure 10 Spray at 603 K, 36 µs after injection, exhibiting vortices at the spray edge.

The widening of the spray resulting from these processes appears to enhance entrainment of air. As the spray continues, the initial fluid is driven forward, flattening out into a mushroom shaped cap at the front of the spray. This drives the bow shock seen in Schlieren imaging discussed prior. Clearly visible vortices form at the edges of these caps, wrapping

back around towards the center of the spray. These turbulent effects serve to further enhance mixing. Both Fig. 9 and Fig. 10 demonstrate these vortices.

This near nozzle data is in agreement with the wider spray trends presented earlier. Trends in spray behavior favorable for improved mixing performance such as wider spray angles and more rapid vaporization are evident for spray conditions in the near-critical and supercritical regimes.

Continuation of this work into a pressurized combustion chamber is the next step in this study. Holding the environment into which fuel is injected beyond the fuel's critical point ought to have interesting effects upon the spray. Working in a constant volume combustion chamber (CVCC) allows for mixing and ignition studies to be carried out in an environment representative of in-cylinder conditions. These studies ought to be carried out making use of a surrogate fuel in place of fuels purchased off the shelf to simplify analysis. Investigation into the interaction of supercritical sprays with other advanced combustion strategies is warranted and may prove an interesting course of study.

## **Conclusions**

Analysis of spray evolution and breakup in the subcritical and near-critical regimes is conducted. Changes in spray parameters consistent with a transition from the traditional spray model of turbulent breakup, atomization, and evaporation towards a diffusion dominated mixing process more akin to a gas jet are investigated. It is shown that the spray evaporates more rapidly as the supercritical region is entered. A marked jump in vapor to liquid ratio is observed in the vicinity of 568 K, indicating more rapid spray vaporization. Increases both in injection pressure and temperature are shown to have a positive effect upon the vapor to liquid ratio, indicating a more rapid spray breakup. Changes in spray structure are shown to be visible in the first microseconds following injector opening as temperature is raised, with a change in plume shape indicative of improved diffusive mixing in the radial direction.

These findings have implications for advanced combustion strategies in compression ignition engines as well as in other high pressure, high temperature fuel injection systems. Combustion chamber and/or injector heating in conjunction with increasing injection pressures has the potential to change the mixing behaviour within the combustion chamber in a manner beneficial to system performance. Taking advantage of this effect would necessitate preheating the entire injection charge, for, as shown in this work, cooling of the fuel negates to some degree the benefits of supercritical fuel injection when fuel is injected into a subcritical ambience.

## Acknowledgement

This material is based upon work supported by, or in part by the National Science Foundation under Grant No. CBET- 2104394. Any opinions, findings, and conclusions or recommendations expressed in this material are those of the author(s) and do not necessarily reflect the views of the funding agencies.

## References

- [1] Morgan, R., Banks, A., Auld, A., Heikal, M., and Lenartowicz, C., "The Benefits of High Injection Pressure on Future Heavy Duty Engine Performance," *SAE Technical Papers*, Vols. 2015-Septe, No. September, 2015.
- [2] Chen, P. C., Wang, W. C., Roberts, W. L., and Fang, T., "Spray and atomization of diesel fuel and its alternatives from a single-hole injector using a common rail fuel

- injection system," Fuel, Vol. 103, No. x, 2013, pp. 850-861.
- [3] Yao, C., Geng, P., Yin, Z., Hu, J., Chen, D., and Ju, Y., "Impacts of nozzle geometry on spray combustion of high pressure common rail injectors in a constant volume combustion chamber," *Fuel*, Vol. 179, 2016, pp. 235–245.
- [4] Yao, C., Hu, J., Geng, P., Shi, J., Zhang, D., and Ju, Y., "Effects of injection pressure on ignition and combustion characteristics of diesel in a premixed methanol/air mixture atmosphere in a constant volume combustion chamber," *Fuel*, Vol. 206, 2017, pp. 593–602.
- [5] Wang, L., Lowrie, J., Ngaile, G., and Fang, T., "High injection pressure diesel sprays from a piezoelectric fuel injector," *Applied Thermal Engineering*, Vol. 152, No. January, 2019, pp. 807–824.
- [6] Huang, W., Wu, Z., Gao, Y., and Zhang, L., "Effect of shock waves on the evolution of high-pressure fuel jets," *Applied Energy*, Vol. 159, 2015, pp. 442–448.
- [7] Kanjanasakul, C., Grisch, F., Saengkaew, S., and Gréhan, G., "Optical characterization of ethane droplets in the vicinity of critical pressure," *Oil and Gas Science and Technology*, Vol. 75, 2020.
- [8] Meinecke, M., Kilzer, A., and Weidner, E., "Background Orientated Schlieren Method Applied for Liquid Systems of Strong Refractive Gradients," *Chemie-Ingenieur-Technik*, Vol. 92, No. 8, 2020, pp. 1089–1097.
- [9] Wang, L., Wang, F., and Fang, T., "Flash boiling hollow cone spray from a GDI injector under different conditions," *International Journal of Multiphase Flow*, Vol. 118, 2019, pp. 50–63.
- [10] Sim, H. S., Yetter, R. A., Connell, T. L., Dabbs, D. M., and Aksay, I. A., "Multifunctional Graphene-Based Additives for Enhanced Combustion of Cracked Hydrocarbon Fuels under Supercritical Conditions," *Combustion Science and Technology*, Vol. 192, No. 7, 2020, pp. 1420–1435.
- [11] Gallarini, S., Cozzi, F., Spinelli, A., and Guardone, A., "Direct velocity measurements in high-temperature non-ideal vapor flows," *Experiments in Fluids*, Vol. 62, No. 10, 2021, pp. 1–18.
- [12] Dahms, R. N., and Oefelein, J. C., "Atomization and dense-fluid breakup regimes in liquid rocket engines," *Journal of Guidance, Control, and Dynamics*, Vol. 38, No. 6, 2015, pp. 1221–1231.
- [13] Yang, D., Chen, L., Zang, J., Huang, Y., and Chen, H., "Experimental characterization and analysis of supercritical jet dynamics by phase-shifting interferometer system," *Journal of Supercritical Fluids*, Vol. 189, No. August, 2022, p. 105724.
- [14] Rezaei, J., Riess, S., and Wensing, M., "Phase change in fuel sprays at diesel engine ambient conditions: Impact of fuel physical properties," *Journal of Supercritical Fluids*, Vol. 170, No. April 2020, 2021, p. 105130.
- [15] Crua, C., Manin, J., and Pickett, L. M., "On the transcritical mixing of fuels at diesel engine conditions," *Fuel*, Vol. 208, 2017, pp. 535–548.
- [16] Klima, T. C., Peter, A., Riess, S., Wensing, M., and Braeuer, A. S., "Quantification of mixture composition, liquid-phase fraction and temperature in transcritical sprays," *Journal of Supercritical Fluids*, Vol. 159, 2020, p. 104777.
- [17] Fu, Q., Zhang, Y., Mo, C., and Yang, L., "Molecular dynamics study on the mechanism of nanoscale jet instability reaching supercritical conditions," *Applied Sciences (Switzerland)*, Vol. 8, No. 10, 2018.
- [18] Gong, Y., Luo, K. H., Ma, X., Shuai, S., and Xu, H., "Atomic-level insights into transition mechanism of dominant mixing modes of multi-component fuel droplets: From evaporation to diffusion," *Fuel*, Vol. 304, No. July, 2021, p. 121464.
- [19] Zhu, H., Battistoni, M., Manjegowda Ningegowda, B., Nadia Zazaravaka Rahantamialisoa, F., Yue, Z., Wang, H., and Yao, M., "Thermodynamic modeling of trans/supercritical fuel sprays in internal combustion engines based on a generalized cubic equation of state," *Fuel*, Vol. 307, No. August 2021, 2022, p. 121894.
- [20] Chung, W. T., Ma, P. C., and Ihme, M., "Examination of diesel spray combustion in supercritical ambient fluid using large-eddy simulations," *International Journal of*

- Engine Research, Vol. 21, No. 1, 2020, pp. 122-133.
- [21] Song, Y., Zheng, Z., Peng, T., Yang, Z., Xiong, W., and Pei, Y., "Numerical investigation of the combustion characteristics of an internal combustion engine with subcritical and supercritical fuel," *Applied Sciences (Switzerland)*, Vol. 10, No. 3, 2020.
- [22] Umemura, A., and Shinjo, J., "A new LES approach to trans-critical mixing and combustion processes in high-pressure liquid-injectant engines," *Proceedings of the Combustion Institute*, Vol. 38, No. 2, 2021, pp. 3107–3129.
- [23] Ju, D., Deng, J., Huang, Z., Xia, J., Qin, H., and Jiang, F., "Large Eddy Simulation with dense fluid approximation and experimental study on the commercial diesel trans-critical injections," *Applied Thermal Engineering*, Vol. 183, No. P1, 2021, p. 116181.
- [24] Riess, S., Rezaei, J., Weiss, L., Peter, A., and Wensing, M., "Phase change in fuel sprays at diesel engine ambient conditions: Modeling and experimental validation," *Journal of Supercritical Fluids*, Vol. 173, No. March, 2021, p. 105224.
- [25] Zhang, H., Yi, P., and Yang, S., "Multicomponent Effects on the Supercritical CO2 Systems: Mixture Critical Point and Phase Separation," *Flow, Turbulence and Combustion*, Vol. 109, No. 2, 2022, pp. 515–543.